Clinical Proteomics

RESEARCH

Open Access

Comprehensive analysis of chronic hepatitis B concurrent with non-alcoholic fatty liver disease: a proteomics report based on clinical liver samples

Xin Tong[1†], Yawen Wan[2†], Shengxia Yin[1†], Li Shao[3,5], Renling Yao[1], Xiaoyan Ma[1], Fajuan Rui[2], Junping Shi[3,5*], Chao Wu[1,2,4*] and Jie Li[1,2,4*]

Abstract

Background and aims In recent years, the prevalence of non-alcoholic fatty liver disease (NAFLD) has risen among patients with chronic hepatitis B (CHB), coinciding with the increasing rates of obesity and metabolic syndrome. Both conditions can contribute to liver fibrosis and even hepatocellular carcinoma; however, the pathogenesis of each disease, as well as CHB concurrent with NAFLD, remains incompletely understood.

Methods We comprehensively analyzed protein levels in liver tissues from four distinct groups: healthy controls, patients with CHB, patients with NAFLD, and those with CHB and NAFLD using proteomic profiling. Subsequently, we performed bioinformatics analyses based on the results of differentially expressed proteins (DEPs). We also verified the levels of select DEPs in both patient liver samples and a murine model.

Results Our investigation revealed that enhanced viral clearance in patients with hepatitis B virus (HBV) with concurrent NAFLD might be associated with an inflammatory response and the activation of numerous metabolic pathways within the body. Meanwhile, the degree of hepatic steatosis was associated with anomalies in fatty acid degradation, glycolysis/gluconeogenesis, and other metabolic processes. However, the prognosis for patients with CHB and concurrent NAFLD may be severe, and this may be connected to the altered levels of proteins such as ACAT1, ACY1, SERPINB3, MTCH2, ALDH2, ECHS1, S100A7, and LRP6.

Conclusion In comparison to CHB and NAFLD alone, the prognosis for CHB complicated by NAFLD appears less favorable. This disparity is closely correlated with distinct protein level patterns in the liver following the onset of both

†Xin Tong, Yawen Wan and Shengxia Yin contributed equally to this work.

*Correspondence:
Junping Shi
20131004@hznu.edu.cn
Chao Wu
dr.wu@nju.edu.cn
Jie Li
lijier@nju.edu.cn

Full list of author information is available at the end of the article

diseases. Our study provides novel insights into the disease progression and clinical mechanisms underlying CHB and NAFLD.

Introduction

Chronic hepatitis B (CHB) is a persistent liver disease induced by the hepatitis B virus (HBV), which remains a significant global threat despite the availability of vaccines and antiviral treatments [1]. CHB afflicts over 250 million individuals worldwide, resulting in more than 800,000 annual fatalities due to the progression of liver disease to cirrhosis and hepatocellular carcinoma (HCC) [2]. Simultaneously, non-alcoholic fatty liver disease (NAFLD) has emerged as another prevalent chronic liver disorder, affecting a quarter of the global population. Recent studies indicate that the worldwide prevalence of NAFLD stands at 29.8% [3]. NAFLD is intricately linked to obesity and includes a spectrum of conditions, including steatosis, non-alcoholic steatohepatitis, fibrosis, cirrhosis, and even HCC [4, 5]. As the prevalence of NAFLD continues to rise, the co-occurrence of NAFLD and HBV infection is also increasing. Approximately 32.8% of patients with CHB are estimated to have NAFLD [6].

Given that both HBV infection and NAFLD can induce chronic liver injury, exacerbate liver damage, increase the risk of cirrhosis and HCC, and profoundly jeopardize liver health, the interplay between these two diseases has garnered substantial attention [7]. However, certain studies suggest that NAFLD is positively associated with reduced HBV serum markers in patients with CHB, who also exhibit a diminished incidence of hyperlipidemia and NAFLD [8]. Despite various speculations, the mechanism underlying the interaction between CHB and NAFLD remains unclear, necessitating further study.

In this study, we aimed to explore the differences in liver protein levels between patients with hepatitis B and coexisting fatty liver and those with CHB and NAFLD as standalone conditions, respectively. We used a data-independent acquisition (DIA) approach for proteomics analysis of liver tissues, evaluating significantly differentially expressed proteins (DEPs) using Gene Ontology (GO) and the Kyoto Encyclopedia of Genes and Genomes (KEGG). We assessed variations in protein levels among patients with CHB, patients with NAFLD, and healthy individuals to identify DEPs potentially implicated in liver tissue. In particular, we conducted differential analysis of liver proteins in patients with CHB concurrently suffering from NAFLD compared to those with CHB and NAFLD alone, with the aim of identifying novel insights into the mechanisms underlying disease interactions. Additionally, we validated our findings in the livers of a murine model, addressing the potential implications of our results for the mechanisms underlying liver diseases, including oxidative stress, metabolic anomalies, and chronic inflammation.

Materials and methods

Participants

The study included healthy controls and eligible patients with either CHB or NAFLD, identified at the Department of Infectious Diseases at Nanjing Drum Tower Hospital in China. Patients who had received treatment with nucleoside analogs or interferons within the past 2 years were excluded from the study. Additionally, patients with concurrent infections, including human immunodeficiency virus, hepatitis A virus, hepatitis C virus (HCV), hepatitis D virus, or other viral infections, were excluded. Those with severe liver conditions, such as cirrhosis or HCC, were also excluded from the study. All participants provided informed consent, and this study was approved by the institutional review board of Nanjing Drum Tower Hospital, conducted in accordance with the Helsinki Declaration and the guidelines of the National Health and Medical Research Council of China.

Liver biopsy

Liver biopsies were conducted using ultrasonography with 16-gauge BARD disposable core biopsy needles (BARD Inc., USA). Samples exceeding 15 mm in length were collected. Skilled liver pathologists, who were unaware of patients' clinical histories, assessed the biopsy tissue. Hepatic histological features, including steatosis grade (0–3) and inflammation grade (0–4), were evaluated using the Brunt criteria. Liver fibrosis was classified according to Scheuer's classification as S0–S4.

Sample preparation

To isolate the most abundant proteins, samples were processed using the Human Multiple Affinity Removal System Column following the manufacturer's protocol (Agilent Technologies). High and low abundance proteins were separately collected, and a 5-kDa ultrafiltration tube (Sartorius) was used to desalinate and concentrate high and low-abundance components. SDT buffer (4% sodium dodecyl sulfate, 100 mM dithiothreitol, 150 mM Tris-HCl, pH 8.0) was added, followed by boiling for 15 min and centrifugation at 14,000 *g* for 20 min. The supernatant was quantified using the Bicinchoninic Acid Protein Assay Kit (Bio-Rad, USA), and the supernatant sample was stored at – 80 °C.

Data-independent acquisition

Peptides from each sample were analyzed by liquid chromatography-mass spectrometry (MS)/MS operating in the DIA mode, conducted by Shanghai Applied Protein Technology Co., Ltd. Each DIA cycle included one full MS-SIM scan, and 30 DIA scans covered a mass range of 350–1800 m/z. The settings were as follows: selected ion monitoring (SIM) full scan resolution was 120,000 at 200 m/z, AGC 3e6, maximum IT 50 ms, profile mode. DIA scans were set at a resolution of 15,000, AGC target 3e6, Max IT auto, and normalized collision energy was set at 30 eV. The runtime was 120 min with a linear gradient of buffer B (84% acetonitrile and 0.1% formic acid) at a flow rate of 250 nl/min. Quality control samples, comprised of an equal aliquot from each sample in the experiment, were injected in the DIA mode at the outset of the MS study and after every 6 injections throughout the experiment to monitor MS performance.

DIA data analysis

DIA data was analyzed using SpectronautTM 14.4.200727.47784, with searches performed against the previously constructed spectral library. Key software parameters were configured as follows: retention time prediction type was dynamic iRT, interference on MS2 level correction was enabled, and cross-run normalization was enabled. All results were subjected to filtering based on a Q-value cutoff of 0.01 (equivalent to false discovery rate < 1%).

Bioinformatic analysis

Significantly DEPs were identified using screening criteria of fold change ≥ 1.5 and $p < 0.05$. Hierarchical clustering was applied to cluster DEPs, and the data were visually represented as heat maps. GO term analysis involved several key processes, including blast, GO mapping, GO annotation, and interproScan for annotation enhancement. Protein differences were quantified using cluster analysis. GO enrichment analysis of DEPs was conducted for biological processes, cellular components, and molecular functions using Blast2Go. Pathway enrichment analysis of protein clusters was performed using the online KEGG database (http://geneontology.org). Enrichment analysis was performed using the Fisher's exact test, with the entire dataset of quantified proteins as the background to assess functional associations between differential proteins. The online tool Search Tool for the Retrieval of Interacting Genes/Proteins (STRING) was used with high confidence (0.70) and for the organism (*Homo sapiens*).

Immunohistochemistry (IHC)

IHC was conducted using routine techniques. In brief, deparaffinized tissue sections were treated with 3% hydrogen peroxide for 10 min at 37 °C. Tissue sections were then subjected to incubation in 0.01 M citrate antigen retrieval solution (pH 6.0), heated at 95 °C in a microwave oven for 10 min, and allowed to cool to room temperature. Slides were incubated for 2 h at room temperature (RT) with primary rabbit polyclonal antibodies, including ACAT1 (Abcam; Rabbit; 1:100 dilution), ACY1 (Abcam; Rabbit; 1:100 dilution), SERPINB3 (Abcam; Rabbit; 1:100 dilution), MTCH2 (Abcam; Rabbit; 1:100 dilution), ALDH2 (Abcam; Rabbit; 1:100 dilution), and ECHS1 (Abcam; Rabbit; 1:100 dilution). Then the slides were incubated in secondary antibodies conjugated with horseradish peroxidase (Rabbit; ZSGB-Bio, China) for 40 min at RT, followed by incubation with the substrate 3,3′-diaminobenzidine (ZSGB-Bio, China), and counterstained with Mayer's hematoxylin. For negative controls, primary antibodies were not added to the dilution buffer. Granular cytoplasmic and/or membranous staining of ACAT1, ACY1, SERPINB3, MTCH2, ALDH2, and ECHS1 were considered positive.

Mouse model

C57BL/6J mice aged 4–5 weeks, acquired from Gempharmatech Co., Ltd. (Nanjing, China), were housed in a clean animal facility at Nanjing University with a 12-h light/12-h dark cycle. Mice received tail vein injections of adenovirus ($0.5–1.0 \times 10^9$ active viral particles in 200 µl of phosphate buffered saline) every 4 weeks. Additionally, mice were either fed a normal chow diet (9% fat; Lab Diet) or a high-fat diet (HFD; 60% fat; Research Diets) and grouped into control, NAFLD, HBV, and NAFLD + HBV groups, there were 4 mice in each group. Weekly body weights and blood glucose levels were recorded. At the end of 6, 12, and 18 weeks, the mice were euthanized, and blood and liver samples were collected for further biochemical analysis. All animal experiments adhered strictly to the guidelines of the Animal Center of Nanjing University, and ethical approval for all animal experimental procedures was obtained from the Experimental Animal Ethical Committee of Nanjing Drum Tower Hospital.

Reverse transcription-quantitative real-time polymerase chain reaction (RT-qPCR)

Total RNA was extracted from mouse livers using a TRIzol-based method (Invitrogen). Total RNA (1 µg) was reverse transcribed with the High-Capacity cDNA Reverse Transcription Kit and random primers (Applied Biosystems). qPCR was conducted using the SYBR Green I qPCR kit (Promega) on a Bio-Rad CFX system. All gene expression data were normalized to 36B4 expression levels. Specific primer sequences are provided in Supplementary Table 1.

Statistical analysis

Continuous parameters were reported as medians (interquartile range), whereas categorical data were presented as counts (proportion). The independent sample T-test (for normal distribution) and Mann–Whitney U test (for non-normal distribution) were employed to compare continuous variables between two groups (*, $p < 0.05$; **, $p < 0.01$; ***, $p < 0.001$).

Results

Clinical characteristics of study population

The study population was classified into four groups, and a comparison of clinical features was conducted among these groups. As shown in Table 1 (at the end of the document text file), the median age was similar, ranging from 35 to 40 years. Patients with CHB had a higher proportion of females (75%), whereas patients with CHB and NAFLD had a higher proportion of males (90%). Patients with NAFLD and CHB concurrent with NAFLD exhibited elevated levels of alanine transaminase (ALT), aspartate aminotransferase (AST), Triglyceride(TG), Total cholesterol(TC),γ-glutamyl transpeptadase(GGT), and Uric Acid(UA) compared to the other two groups. These characteristics were comparable between the latter two groups. The groups of CHB and CHB concurrent with NAFLD were significantly positive for HBeAg, HBsAg, and HBV-DNA, although these markers showed no significant differences between the two groups.

Quantitative protein detection

DIA mass spectrometry was employed to create and analyze a spectral library of human liver proteins derived from 31 subjects, including 8 patients with CHB, 7 patients with NAFLD, 10 patients with CHB and concurrent NAFLD, and 6 healthy individuals. This analysis resulted in the identification of 21,430 peptides and 3,199 proteins (Fig. 1A-B). Compared with the healthy control group, a total of 170 and 100 proteins were found to be differentially expressed in the CHB and NAFLD groups, respectively. Among these DEPs, 51 were upregulated and 129 were downregulated in the CHB group, whereas 80 were upregulated and 20 were downregulated in the group NAFLD. When comparing the CHB group to the group of patients with CHB and NAFLD, a total of 109 proteins were differentially expressed, with 73 being upregulated and 36 downregulated. In comparison to the NAFLD group, a total of 221 proteins were differentially expressed in the group of CHB patients with NAFLD, comprising 22 upregulated and 199 downregulated proteins (Fig. 1C). Among the liver proteins identified, 135 were exclusively detected in CHB samples, 37 were exclusive to NAFLD samples, and only 12 were exclusively present in the samples from patients with CHB

Table 1 Demographic and epidemiologic characteristics of patients

Variables (*n* [%] or median [IQR])	HC (*n* = 6)	CHB(*n* = 8)	NAFLD(*n* = 7)	CHB + NAFLD(*n* = 10)	*p* value
Age (ys)	35	39.00(31.25–42.25)	36.00(28.00–43.00)	35.50(33.25–39.25)	
Sex					
Female (%)	2 (33.3)	6 (75)	5 (71.4)	1 (10)	
Male(%)	4 (66.7)	2 (25)	2 (28.6)	9 (90)	
BMI	22.32(19.96–25.36)	21.88(19.82–24.36)	42.72(35.50-44.22)	25.86(23.20-27.52)	*1
Blood routine					
AST(U/L)	20.68(16.34–26.12	19.55(14.28–24.80)	38.80(16.90–64.00)	31.30(23.1-40.28)	*1
ALT(U/L)	16.40(14.80-30.54)	17.40(14.40-34.13)	48.55(39.78–62.98)	61.90(37.00-76.70)	*1
TG(mmol/L)	0.89(0.69–1.13)	0.77(0.66–0.90)	1.92(1.44–2.60)	1.91(1.35–3.04)	**1
TC(mmol/L)	4.19(3.19–5.12)	4.39(3.89–5.15)	5.81(4.48–6.15)	4.88(3.96–5.01)	*1
HDL (mmol/L)	1.78(1.17–1.61)	1.56(1.27–1.78)	1.04(0.99–1.06)	0.87(0.72–1.09)	
LDL(mmol/L)	2.49(2.05–2.68)	2.49(2.05–2.68)	4.03(2.47–4.51)	3.15(2.25–3.29)	
GGT(U/L)	15.78(12.44–27.85)	13.65(11.43–18.65)	61.60(38.70-104.10)	49.60(27.98–72.55)	*1
UA (μmol/L)	310.50(230.00-359.00)	270.50(227.00-330.00)	439.00(401.00-533.00)	435.00(383.00-510.25)	*1
ALP(U/L)	45.35(41.24-68.215)	48.35(40.25-63.975)	84.90(59.60-105.10)	63.90(53.40-86.78)	
ALB (g/L)	42.97(40.33–44.46)	43.05(40.28–47.08)	44.00(40.90–45.50)	43.60(41.58–45.23)	
FBG (mmol/L)	4.05(3.43–4.74)	4.27(3.83–4.45)	6.13(5.49–7.61)	4.33(4.15–4.63)	*2
TB (μmol/L)	8.90(6.50–11.30)	14.90(7.50-15.88)	12.95(9.50–15.30)	8.70(5.80–10.70)	
HBsAg(log_{10}IU/mL)		3.86(2.93–4.48)	0	3.68(2.29–4.25)	
HBeAg positive(%)		5(62.5)	0	8(80)	
HBV-DNA(log_{10}IU/mL)		3.90(3.32–7.93)	0	3.26(2.86–5.06)	

Notes 1:CHB and CHB + NAFLD; 2:NAFLD and CHB + NAFLD.*, $p < 0.05$; **, $p < 0.001$

Abbreviations ALT, alanine transferase; AST, aspartate transferase; TG, triglyceride; TC, total cholesterol; HDL, high density lipoprotein; LDL, low density lipoprotein; ALP, alkaline phosphatase; GGT, γ-Glutamyl transferase; TB, total bilirubin; ALB, albumin; HBeAg, hepatitis B e antigen; HBsAg, hepatitis B s antigen; UA, uric acid; FBG, asting blood glucose

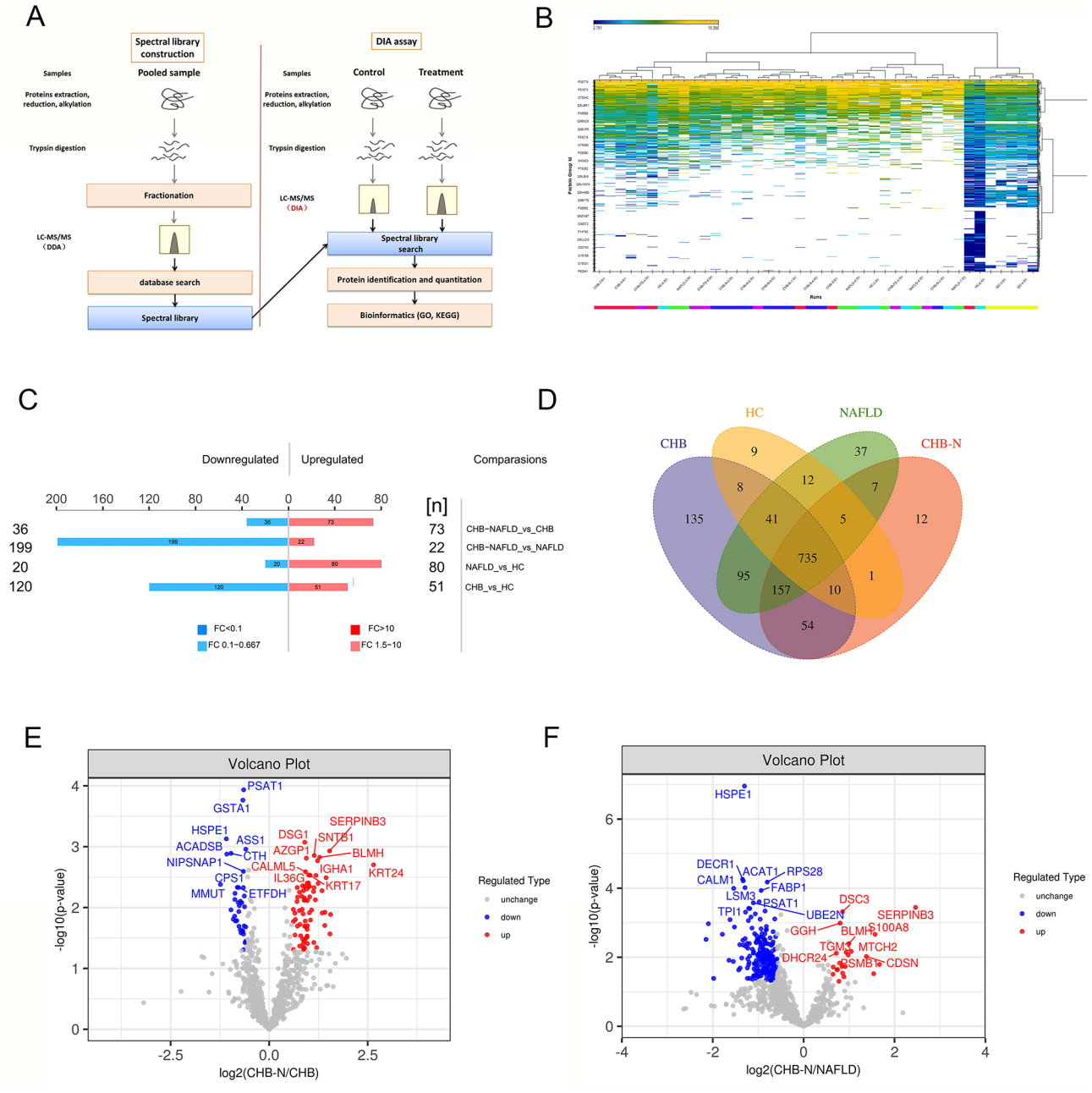

Fig. 1 Liver protein identification by the DIA for patients in the HC, CHB, NAFLD, CHB concurrent with NAFLD. (**A**) DIA Experimental Procedure. (**B**) Quantitative heatmap of total DIA identified proteins for all samples. (**C**) Histogram of quantitative protein difference results. (**D**) The Venn diagrams show the numbers of identified proteins and the overlaps of protein identification in the 4 groups. (**E**) Volcano plot representing the protein abundance changes (groups CHB vs. CHB-NAFLD) (**F**) Volcano plot representing the protein abundance changes (groups NAFLD vs. CHB-NAFLD)

and NAFLD. A total of 735 proteins overlapped among the four groups, accounting for 52% of the total quantified proteins (Fig. 1D). To highlight the most significantly dysregulated proteins in patients with CHB and NAFLD compared to patients with only CHB and those with only NAFLD, the top 10 most significant differences in upregulated and downregulated proteins were marked on the volcano plot, using fold change and p-value T-test criteria (Fig. 1E and F).

GO enrichment analysis and protein structural domains analysis

Based on these results, we generated GO functional classification maps to compared with standalone CHB, dysregulated proteins in patients with CHB concurrent with NAFLD were associated with processes such as keratinocyte differentiation, epidermal cell differentiation, growth, immunoglobulin complex, and homocysteine metabolic processes. Notably, proteins that were

significantly dysregulated between the two groups were primarily enriched in biological processes such as multicellular organismal processes, cellular developmental processes, and cellular amino acid biosynthetic processes (Fig. 2B). In general, protein interactions are often structured in terms of structural domains, and changes in amino acids or modifications within these domains can lead to alterations in key protein functions. The analysis of structural domain enrichment for DEPs indicated that the top five most enriched structural domains were intermediate filament protein, keratin type II head, FAD-dependent oxidoreductase central domain, serpin (serine protease inhibitor), and immunoglobulin V-set domain (Fig. 2A).

The GO enrichment analysis of biological functions related to the proteins that exhibited differential abundance in NAFLD versus CHB concurrent with NAFLD indicated that the CHB concurrent with NAFLD group

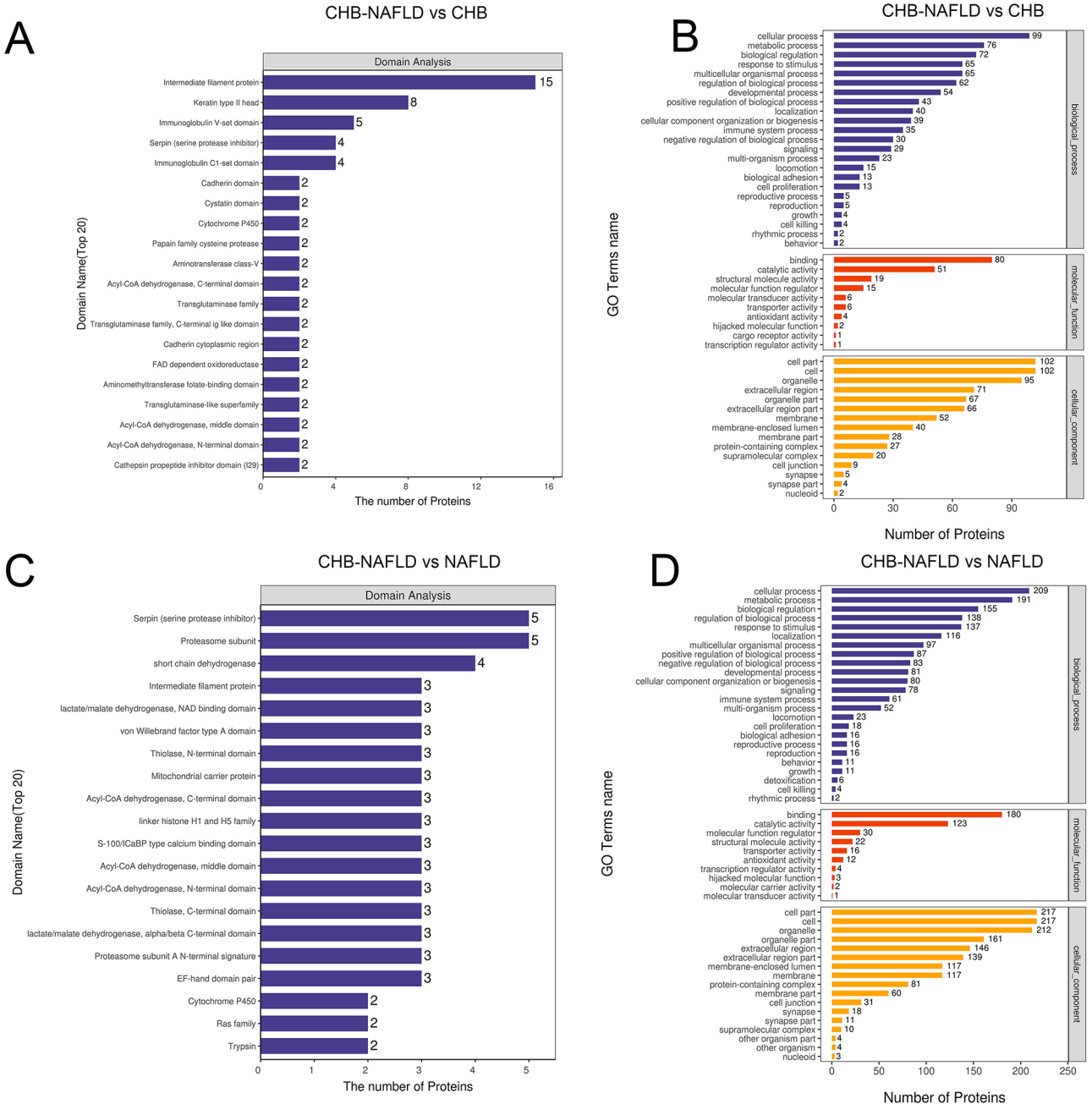

Fig. 2 (**A**) Histogram of structural domain analysis of differentially expressed proteins in CHB-NAFLD vs. CHB group. (**B**) The histograms in gene ontology (GO) analysis of the differentially expressed proteins in CHB-NAFLD vs. CHB. (**C**) Histogram of structural domain analysis of differentially expressed proteins in CHB-NAFLD vs. NAFLD group. (**D**) The histograms in GO analysis of the differentially expressed proteins in CHB-NAFLD vs. NAFLD group

was enriched in proteins associated with various essential processes. These processes included cellular metabolic processes, organic substance metabolic processes, small molecule metabolic processes, carboxylic acid metabolic processes, and cellular catabolic processes. Functionally, these proteins were primarily associated with antioxidant activity, long-chain fatty acid binding, fatty acid binding, and endopeptidase regulator activity. They were primarily localized in the extracellular organelle, extracellular vesicle, and the extracellular region (Fig. 2C and D).

KEGG pathway analysis

In addition, KEGG pathway analysis revealed that DEPs in patients were enriched in various biological pathways within KEGG categories. Upregulated proteins were annotated in three major pathways: *Staphylococcus aureus* infection, the estrogen signaling pathway, and cholesterol metabolism. Conversely, downregulated proteins were annotated in 17 major pathways, with the top three most enriched pathways being valine, leucine and isoleucine degradation, glycine, serine, and threonine metabolism, and butanoate metabolism (Fig. 3A and B). Moreover, propanoate and beta-alanine metabolism, as well as fatty acid degradation, were among the main KEGG pathways related to the differential proteins between the two groups. The differences in various metabolism-related pathways in the livers of patients with CHB concurrent with fatty liver were more pronounced compared to those with standalone CHB, especially with regards to the abnormal activation of

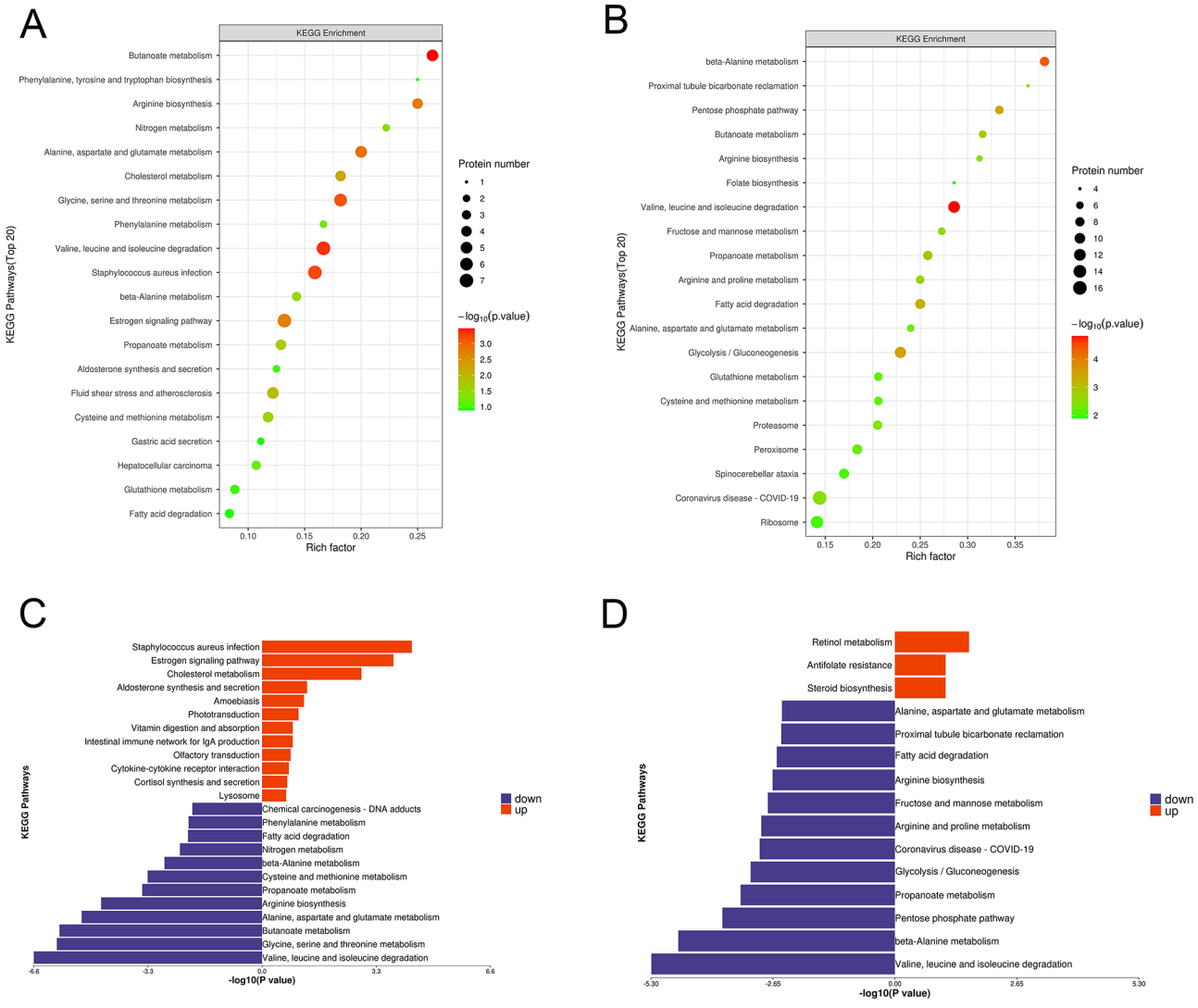

Fig. 3 (**A**) KEGG pathway enrichment bubble map of differentially expressed proteins in CHB vs. CHB-NAFLD group. (**B**) KEGG pathway enrichment bubble map of differentially expressed proteins in NAFLD vs. CHB-NAFLD group. (**C**) Pathway enrichment butterfly plots of up- and down-regulated differential proteins in the CHB vs. CHB-NAFLD group. (**D**) Pathway enrichment butterfly plots of up- and down-regulated differential proteins in the NAFLD vs. CHB-NAFLD group

cholesterol metabolic pathways, which aligns with the characteristics of fatty liver disease. These changes were primarily associated with the differential enrichment of proteins such as KRT24, SERPINB3, MTCH2, CDSN, SYPL1, AGXT, peroxisome proliferator-activated receptor-gamma coactivator (PGC1-α), and others. Furthermore, after the development of concurrent fatty liver, pathways that were abnormally regulated in CHB alone were instead inhibited. For instance, the glycine, serine, and threonine metabolism pathways were abnormally activated in the CHB group compared to healthy subjects, but they were inhibited in the CHB concurrent with NAFLD group when compared to patients with CHB alone. This inhibition was associated with a decrease in CBS, PSAT1, AGXT, CTH, DMGDH, and SARDH after CHB concurrent with NAFLD (Figure S1). Meanwhile, the interleukin (IL)-17 signaling pathway was activated in the CHB concurrent with NAFLD group compared to the standalone CHB group, primarily associated with the increased expression of S100A7 (Figure S2), known to promote the innate immune response of the host. These findings suggest that the development of CHB may be inhibited after the occurrence of concurrent NAFLD. Interestingly, the CHB concurrent with NAFLD group exhibited the suppression of the HCC pathway compared to the group with CHB alone, and this suppression was associated with elevated LRP6 expression (Figure S3).

Using the KEGG pathway database, KEGG analysis of the NAFLD versus CHB concurrent with NAFLD group revealed 8 major upregulated pathways, including metabolism of xenobiotics by cytochrome P450, IL-17 signaling pathway, and retinol metabolism. In contrast, 36 major pathways were downregulated, including valine, leucine, and isoleucine degradation, beta-alanine metabolism, pentose phosphate pathway, propanoate metabolism, glycolysis/gluconeogenesis, fatty acid degradation, peroxisome proliferator-activated receptor (PPAR) signaling pathway, and fat digestion and absorption. These findings shed light on the inhibition of numerous metabolic pathways in patients with NAFLD in combination with HBV infection, offering new insights into the interaction mechanisms between the two diseases (Fig. 3C and D). Notably, following concurrent HBV infection, pathways that were previously abnormally activated in patients with NAFLD alone were instead inhibited. For instance, glycolysis/gluconeogenesis, pyruvate metabolism, fatty acid degradation, and fat digestion and absorption were abnormally activated in the NAFLD group compared to healthy subjects but were inhibited in the group with CHB and concurrent NAFLD when compared to patients with NAFLD (Figure S4). Key DEPs responsible for these changes included ACADM, ECHS1, ACAT1, EHHADH, and ALDH2. Further confirmation through IHC revealed a significant decrease in positive staining for ECHS1, ACAT1, and ALDH2 after the onset of both diseases.

Validation of dysregulated protein expression in patient liver tissues

The alterations in DEPs were validated at the protein level through IHC, using liver samples from patients (3 from healthy controls, 3 from patients with CHB, 3 from patients with NAFLD, and 3 from patients with CHB + NAFLD). In particular, we assessed three key proteins highlighted in the previously mentioned analyses. Our results confirmed a significant increase in hepatic SERPINB3, ACY1, and MTCH2 positive staining in patients with CHB concurrent with NAFLD compared to patients with CHB alone (Fig. 4A). Conversely, we observed reduced protein levels of hepatic ACAT1, ECHS1, and ALDH2 in patients with CHB and NAFLD compared to patients with NAFLD alone (Fig. 4B). These findings provide valuable insights for future investigations into CHB concurrent with NAFLD, although further study is required to explore the underlying molecular mechanisms.

Validation of dysregulated proteins in mouse models

To validate the proteomic results in mouse models, we generated mouse models for HBV, NAFLD, and NAFLD with HBV infection (Fig. 5A). Hepatic hematoxylin and eosin staining revealed reduced hepatocyte volumes, fewer dispersed lipid vacuoles, and compressed liver sinusoids in NAFLD + HBV mice compared to those in NAFLD mice (Fig. 5B). Additionally, we found that the body weight of the NAFLD + HBV group was decreased compared to the NAFLD group, whereas the blood glucose levels did not significantly change in either group (Fig. 5C). Notably, reduced TG and TC secretion levels were identified in NAFLD + HBV mice compared to NAFLD mice (Fig. 5D). Moreover, the serum levels of HBsAg, HBeAg, and HBV-DNA were significantly decreased after 12 weeks of HFD compared to the NAFLD group. Conversely, both serum ALT, AST, triglycerides, and cholesterol in the NAFLD + HBV group were higher than in the NAFLD group, whereas the HBV and control groups exhibited no significant change (Fig. 5E). Furthermore, based on the results of previous analyses, we selected multiple genes involved in hepatic lipogenesis and infection, and examined their expression using qRT-PCR (Fig. 5F).

Discussion

As both CHB and NAFLD represent increasingly common liver diseases, it is essential to study not only the mechanisms underlying these diseases individually but also the interactions between the two. The application of proteomic analysis through DIA mass spectrometry is a

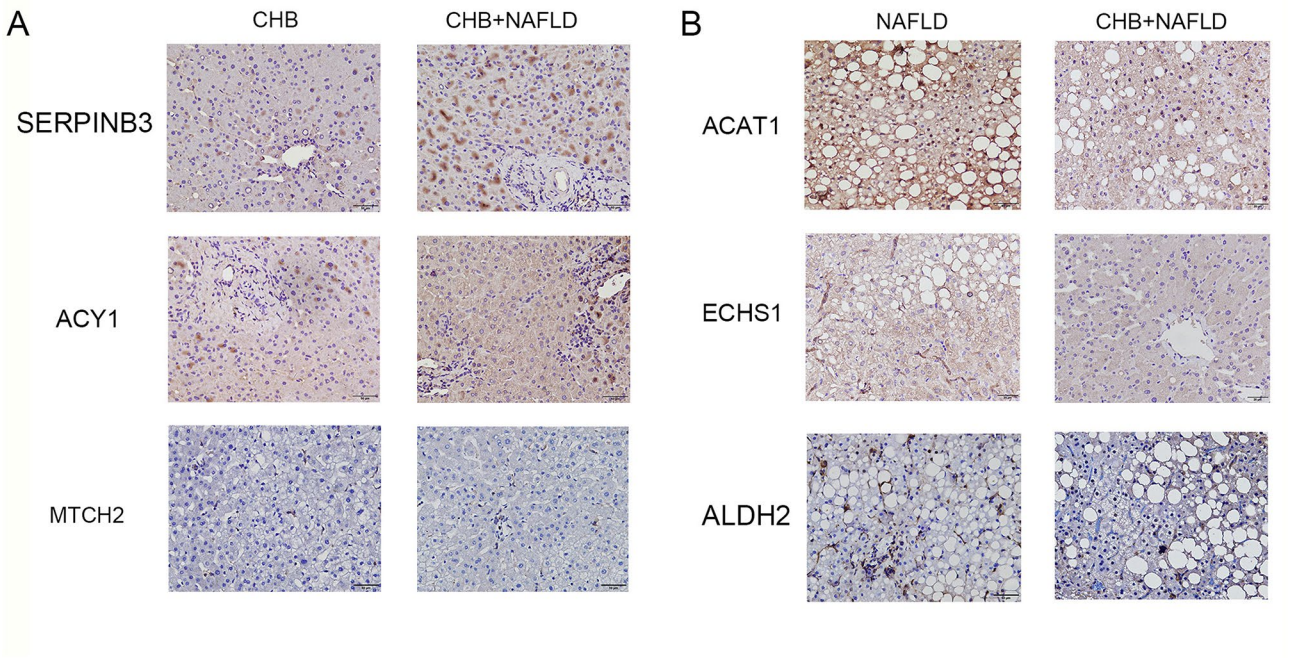

Fig. 4 (**A**) Verification of differential proteins between the CHB vs. CHB-NAFLD group by immunohistochemistry. (**B**) Verification of differential proteins between the NAFLD vs. CHB-NAFLD group by immunohistochemistry (Scale bar: 50 μm)

robust method for providing comprehensive insights into global protein expression with high precision. Using this platform, our dataset has revealed significant differences in protein levels across four groups of liver specimens: healthy subjects, patients with only CHB, patients with only NAFLD, and patients with CHB and concurrent NAFLD.

HBV, a small hepatotropic DNA virus, can persist and lead to chronic necro-inflammatory liver diseases. Because HBV is largely noncytopathic, it is believed that the host immune response plays a major role in HBV-associated diseases [9]. The disappearance of HBsAg and undetectable HBV-DNA in the serum of patients with CHB signify important hallmarks of functional cure [10]. Recent studies have indicated that HBsAg clearance and HBV-DNA suppression are positively correlated [11, 12]. In our previous research, we observed that patients with CHB and NAFLD were significantly more likely to be HBeAg negative (74.3% vs. 62.8%) compared to patients with CHB without NAFLD [13]. The potential mechanistic role of NAFLD in HBV infection remains unclear, with several speculations. Some studies suggest that metabolic factors in NAFLD may influence HBV replication. For example, Shlomai et al. revealed that the metabolic alterations induced by NAFLD may inhibit HBV replication by suppressing the level of PGC-1α [14]. Our results validate this hypothesis by revealing decreased levels of PGC-1α in the livers of patients with CHB + NAFLD compared to patients with CHB alone in the proteomic analysis of patient livers and in the livers of model mice. This increase in PGC-1α inhibits the replication of HBV-DNA, subsequently affecting the development of CHB. The observed variations in various metabolism-related pathways in the livers of patients with CHB concurrent with NAFLD were more pronounced than in those with standalone CHB. For instance, the glycine, serine, and threonine metabolism pathways were abnormally activated in the CHB group compared to healthy subjects, but were inhibited in the group with CHB and concurrent NAFLD when compared to patients with CHB alone. Whether these differences in metabolic levels contribute positively to HBV clearance remains unreported in current studies and warrants further exploration.

The occurrence of fatty liver may accelerate HBV clearance in patients with hepatitis B; however, the concurrent occurrence of hepatitis B and fatty liver is harmful to patients. The present results revealed abnormal increases in the levels of proteins associated with *Staphylococcus aureus* infection, cholesterol metabolism, and aldosterone synthesis and secretion, such as SERPINB3, IGHA1, and DSG1, in the liver of patients with CHB concurrent with NAFLD compared with those in the liver of patients suffering from CHB without NAFLD. SERPINB3 levels progressively increase in chronic liver diseases, dysplastic nodules, and hepatocellular carcinoma [15]. Another study reported IGHA1 upregulation in patients with advanced cirrhosis compared with that in matched controls, and this upregulation was associated with HCV

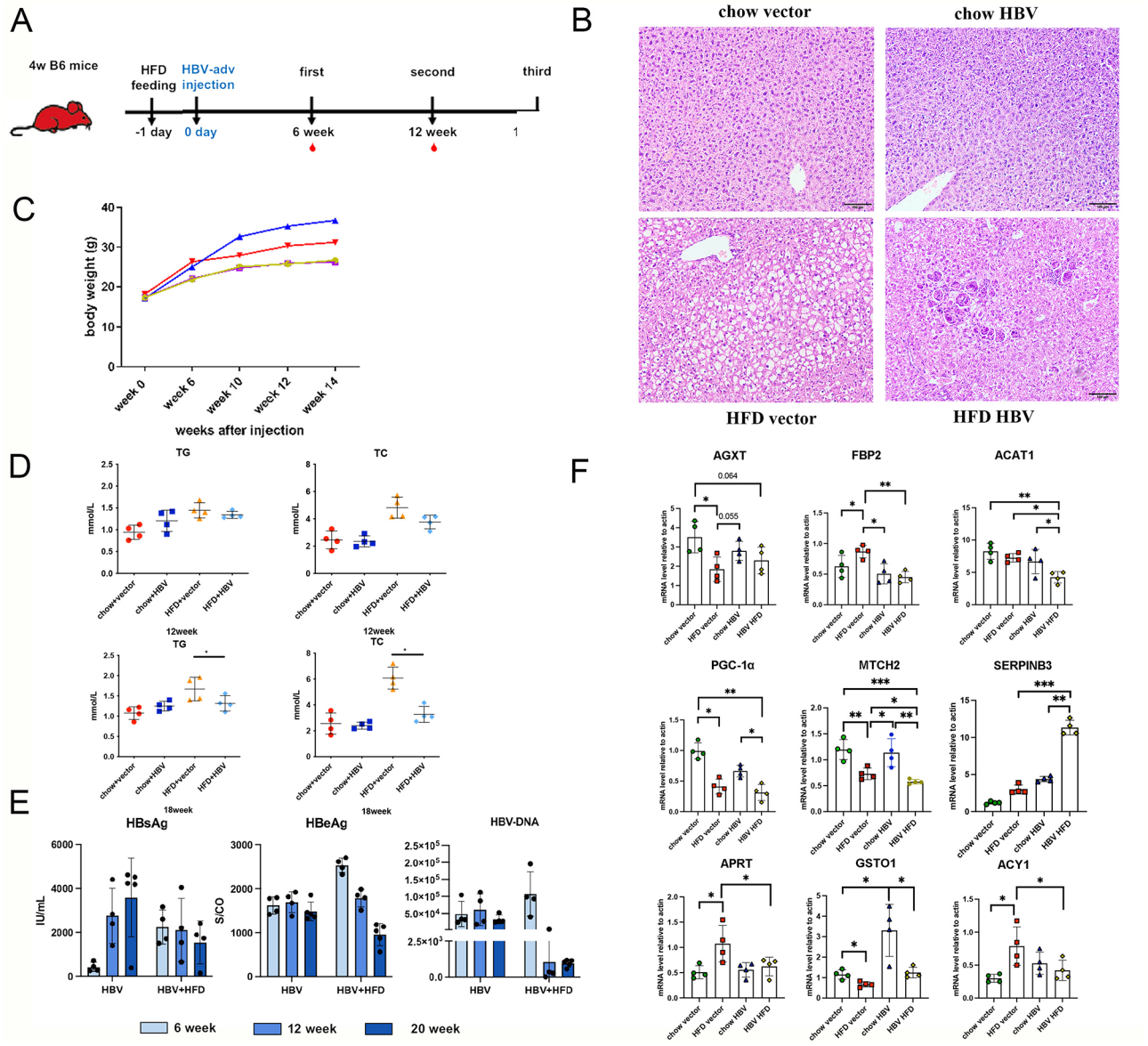

Fig. 5 (**A**) Establishment of mouse models of HBV, NAFLD and NAFLD combined with HBV infection. (**B**) HE staining of liver tissues (**C**) Changes in body weight of mice over time (**D**) Serum TG and TC secretion levels in four groups of mice (**E**) Serum levels of HBsAg, HBeAg and HBV-DNA of mice (**F**) Validation of differential gene expression by qRT-PCR

infection [16]. These findings may suggest that patients with combined hepatic steatosis suffer from activated cirrhosis and possess HCC-associated genes compared with those suffering from hepatitis B alone, which may lead to a poorer prognosis. Moreover, the present findings showed the activated IL-17 signaling pathway in the CHB concurrent with NAFLD group, and a previous study reported that this pathway was involved in the inflammatory response [17], in which high S100A7 and S100A8 expression was associated with the development of various tumors [18, 19]. These outcomes suggest a factor potentially responsible for adverse disease progression after HBV infection concurrent with fatty liver.

Conversely, to date, various studies have indicated that HBV may exert a protective effect on fatty liver development. Even after adjusting for possible confounders and metabolic factors, a significant negative correlation between HBV infection and NAFLD was observed in a study [20]. Additionally, hepatic steatosis in patients with CHB was associated with host metabolic factors [21]. The present DIA results revealed that the levels of proteins related to lipid metabolism, including ACAA2, HADHA, and ECHS1, decreased significantly in patients with hepatitis B concurrent with fatty liver compared with those with fatty liver alone. Furthermore, the KEGG pathways enriched with the DEPs, including fatty acid degradation,

PPAR signaling pathway, and fat digestion and absorption, indicated that specific metabolic alterations in the liver of patients with hepatitis B affected hepatic steatosis and thus the occurrence of CHB concurrent with fatty liver disease; however, the underlying mechanisms need further investigation. Mustafa et al. identified a significant upregulation of a lipid-biosynthesis-related gene in the liver of HBV transgenic mice [22]. Bulent et al. found that in HBV-infected patients, hepatic steatosis was primarily associated with metabolic factors, such as obesity, insulin resistance, and dyslipidemia, rather than viral factors [23]. Herein, significant changes were observed in the levels of proteins such as AGT, which were closely related to insulin resistance, and this finding is consistent with previous findings. Additionally, the differential expression of PGM1, FBP1, ALDA, and ADH1A resulted in changes in glycolysis/gluconeogenesis and associated pathways, suggesting that CHB affected gluconeogenesis and lipid metabolism. This finding provides a basis for future studies.

The present study has several limitations. We analyzed six or seven specimens for each group; however, the sample size of each group was relatively small. Currently, we have not studied the underlying disease mechanism in depth. Additionally, the protein levels and mRNA levels of some results did not match, and the levels of liver-associated proteins in patients and model mice differed. Thus, the mentioned results need further validation and analysis.

In conclusion, we performed the proteomics analysis of livers of healthy controls and patients with CHB, NAFLD, and CHB concurrent with NAFLD and found that accelerated viral clearance in HBV-infected patients with concurrent fatty liver might be associated with an inflammatory response and the activation of many metabolic reactions in the organism. Moreover, the hepatic steatosis level was associated with abnormalities in fatty acid degradation and glycolysis/gluconeogenesis; however, the prognosis of CHB concurrent with NAFLD was probably prolonged. The present study provides new ideas for understanding the development of the two diseases and their interactions.

Abbreviations

CHB	Chronic hepatitis B
HBV	Hepatitis B virus
HCV	Hepatitis C virus
HCC	Hepatocellular carcinoma
NAFLD	Nonalcoholic fatty liver disease
NASH	Non-alcoholic steatohepatitis
ALT	Alanine transaminase AST: aspartate aminotransferase
TG	Triglyceride
TC	Total cholesterol
GGT	γ-glutamyl transpeptadase
UA	Uric Acid
HBeAg	Hepatitis B e antigen
HBsAg	Hepatitis B s antigen
DEPs	Differentially expressed proteins
GO	Gene Ontology
KEGG	Kyoto Encyclopedia Genes and Genomes
DIA	Data-independent acquisition
IHC	Immunohistochemistry
RT-qPCR	Reverse transcription-Quantitative real-time polymerase chain reaction
ACAT1	Acetyl-CoA Acetyltransferase 1
ACY1	Aminoacylase 1
SERPINB3	Serpin Family B Member 3
MTCH2	Mitochondrial Carrier 2
ALDH2	Aldehyde Dehydrogenase 2 Family Member
ECHS1	Enoyl-CoA Hydratase, Short Chain 1
KRT24	Keratin 24
CDSN	Corneodesmosin
SYPL1	Synaptophysin Like 1
AGXT	Alanine-Glyoxylate Aminotransferase
PGC1-α	PPARG Coactivator 1 Alpha
CBS	Cystathionine Beta-Synthase
PSAT1	Phosphoserine Aminotransferase 1
S100A7	S100 Calcium Binding Protein A7
LRP6	LDL Receptor Related Protein 6
ACADM	Acyl-CoA Dehydrogenase Medium Chain
CTH	Cystathionine gamma-lyase
DMGDH	Dimethylglycine dehydrogenase
SARDH	Sarcosine dehydrogenase
EHHADH	Enoyl-CoA Hydratase And 3-Hydroxyacyl CoA Dehydrogenase

Supplementary Information

The online version contains supplementary material available at https://doi.org/10.1186/s12014-024-09523-3.

Supplementary Material 1

Supplementary Material 2

Supplementary Material 3

Supplementary Material 4

Supplementary Material 5

Supplementary Material 6

Supplementary Material 7

Acknowledgements
Not applicable.

Author contributions
All authors contributed to the study conception and design. Material preparation were performed by L.J. and W.C. data collection and analysis were performed by T.X., Y. S. and S.L. Animal experiments were done by performed by W.Y., T.X. and R.F. The first draft of the manuscript was written by T.X. and all authors commented on previous versions of the manuscript. All authors reviewed the manuscript.

Funding
Dr. Jie Li wishes to acknowledge the support from the Noncommunicable Chronic Diseases-National Science and Technology Major Project (No. 2023ZD0508802), The National Natural Science Foundation of China (No. 82170609, 81970545), NSFC-RGC Forum for Young Scholars (No. 82411560273) and the Natural Science Foundation of Jiangsu Province (No. BK20231118).

Data availability
No datasets were generated or analysed during the current study.

Declarations

Ethics approval and consent to participate
This study was approved by the institutional review board of Nanjing Drum Tower Hospital in accordance with the Helsinki Declaration and guidelines

of the Nation Health and Medical Research Council of China. All animal experimental procedures were approved by the Experimental Animal Ethical Committee of Nanjing Drum Tower Hospital.

Consent for publication
Not applicable.

Competing interests
The authors declare no competing interests.

Author details
[1]Department of Infectious Diseases, Nanjing Drum Tower Hospital, Affiliated Hospital of Medical School, Nanjing University, No. 321 Zhongshan Road, Nanjing, Jiangsu 210008, China
[2]Department of Infectious Diseases, Nanjing Drum Tower Hospital Clinical College of Nanjing University of Chinese Medicine, Nanjing, Jiangsu, China
[3]Department of Infectious & Hepatology Diseases, The Affiliated Hospital of Hangzhou Normal University, Hangzhou, Zhejiang, China
[4]Institute of Viruses and Infectious Diseases, Nanjing University, Jiangsu, China
[5]School of Clinical Medicine, Hangzhou Normal University, The Affiliated Hospital of Hangzhou Normal University, Zhejiang 311121, China

Received: 21 December 2023 / Accepted: 23 December 2024
Published online: 13 May 2025

References

1. Polaris Observatory C. Global prevalence, treatment, and prevention of hepatitis B virus infection in 2016: a modelling study. Lancet Gastroenterol Hepatol. 2018;3(6):383–403.
2. Shi Y, Zheng M. Hepatitis B virus persistence and reactivation. BMJ. 2020;370:m2200.
3. Le MH et al. 2019 Global NAFLD Prevalence: A Systematic Review and Meta-analysis. Clin Gastroenterol Hepatol, 2022. 20(12): pp. 2809–2817 e28.
4. Sanyal AJ, et al. Prospective study of outcomes in adults with nonalcoholic fatty liver disease. N Engl J Med. 2021;385(17):1559–69.
5. Powell EE, Wong VW, Rinella M. Non-alcoholic fatty liver disease. Lancet. 2021;397(10290):2212–24.
6. Zheng Q, et al. Systematic review with meta-analysis: prevalence of hepatic steatosis, fibrosis and associated factors in chronic hepatitis B. Aliment Pharmacol Ther. 2021;54(9):1100–9.
7. Chan AW, et al. Concurrent fatty liver increases risk of hepatocellular carcinoma among patients with chronic hepatitis B. J Gastroenterol Hepatol. 2017;32(3):667–76.
8. Tong X, et al. Clinical impact and mechanisms of hepatitis B virus infection concurrent with non-alcoholic fatty liver disease. Chin Med J (Engl). 2022;135(14):1653–63.
9. Tang LSY, et al. Chronic Hepatitis B infection: a review. JAMA. 2018;319(17):1802–13.
10. Lok AS, et al. Hepatitis B cure: from discovery to regulatory approval. Hepatology. 2017;66(4):1296–313.
11. Chu CM, Lin DY, Liaw YF. Does increased body mass index with hepatic steatosis contribute to seroclearance of hepatitis B virus (HBV) surface antigen in chronic HBV infection? Int J Obes (Lond). 2007;31(5):871–5.
12. Chu CM, Lin DY, Liaw YF. Clinical and virological characteristics post HBsAg seroclearance in hepatitis B virus carriers with hepatic steatosis versus those without. Dig Dis Sci. 2013;58(1):275–81.
13. Chang JW, et al. No influence of hepatic steatosis on the 3-year outcomes of patients with quiescent chronic hepatitis B. J Viral Hepat. 2021;28(11):1545–53.
14. Mansouri A, Gattolliat CH, Asselah T. Mitochondrial dysfunction and signaling in Chronic Liver diseases. Gastroenterology. 2018;155(3):629–47.
15. Pontisso P. Role of SERPINB3 in hepatocellular carcinoma. Ann Hepatol. 2014;13(6):722–7.
16. Safaei A, et al. Proteomic study of advanced cirrhosis based on HCV to reveal potential biomarkers. Gastroenterol Hepatol Bed Bench. 2020;13(Suppl1):S113–21.
17. Mills KHG. IL-17 and IL-17-producing cells in protection versus pathology. Nat Rev Immunol. 2023;23(1):38–54.
18. Chen Y, et al. S100A8 and S100A9 in Cancer. Biochim Biophys Acta Rev Cancer. 2023;1878(3):188891.
19. Padilla L, et al. S100A7: from mechanism to cancer therapy. Oncogene. 2017;36(49):6749–61.
20. Joo EJ, et al. Hepatitis B virus infection and decreased risk of nonalcoholic fatty liver disease: a cohort study. Hepatology. 2017;65(3):828–35.
21. Hsu CS, et al. Impact of hepatitis B virus infection on metabolic profiles and modifying factors. J Viral Hepat. 2012;19(2):e48–57.
22. Hajjou M, et al. cDNA microarray analysis of HBV transgenic mouse liver identifies genes in lipid biosynthetic and growth control pathways affected by HBV. J Med Virol. 2005;77(1):57–65.
23. Yilmaz B, et al. Chronic hepatitis B associated with hepatic steatosis, insulin resistance, necroinflammation and fibrosis. Afr Health Sci. 2015;15(3):714–8.

Publisher's note